

DiSHA: Dimension-Sharding Adaptation of Large Language Models with Fast Convergence and Fast Computation

Jiale Kang¹

Abstract

Low-Rank Adaptation (LoRA), a prominent technique within the framework of Parameter-Efficient Fine-Tuning (PEFT), efficiently reduces the computational burden associated with adapting Large Language Models (LLMs) to downstream tasks, thereby enabling resource-constrained fine-tuning. However, existing researches have shown that LoRA suffers from slow convergence. To address this limitation, we introduce Dimension-Sharding Adaptation (DiSHA), which expands the PEFT design space to even fewer trainable parameters and faster convergence. Within DiSHA’s design space, we propose Block Affine Efficient Computation (Bone), a computationally efficient structure that delivers both high performance and efficiency. While certain DiSHA configurations may result in colinear updates to weight shards, we address this with Block Affine Transformation (Bat), a nonlinear variant of DiSHA. Bat introduces nonlinearity by combining trainable matrices with original weight shards in a nonlinear manner, inducing nonlinearity in matrix updates without introducing additional parameters. Empirical results show that Bone, under the DiSHA framework, consistently outperforms LoRA variants in both Natural Language Understanding and Natural Language Generation tasks, with significantly improved computational efficiency. Further analysis demonstrates that BAT enhances model capabilities by leveraging its nonlinear design.

🔗 <https://github.com/JL-er/DiSHA>
 📄 <https://github.com/huggingface/peft>

^{*}Equal contribution ¹RWKVOS. Correspondence to: Jiale Kang <jiale@rwkvos.com>.

1. Introduction

The emergence of Large Language Models (LLMs) has fundamentally transformed many traditional technologies (Radford et al., 2019; Raffel et al., 2020). However, general-purpose large models often struggle to meet the needs of all downstream tasks, making it necessary to fine-tune base models for specific scenarios. Full-scale fine-tuning of large models is computationally costly. As a result, numerous Parameter-Efficient Fine-Tuning (PEFT)(Xu et al., 2023) techniques and quantization methods have emerged to reduce the training costs of large models. Low-Rank Adaptation(LoRA) (Hu et al., 2021) has become one of the most popular PEFT methods due to its small tunable parameter size, its effectiveness, and the possibility of zero inference overhead after fine-tuning. The figure 3 illustrates the structure visualization. However, extensive ex-

periments (Ding et al., 2023; Liu et al., 2024b; Biderman et al., 2024) have shown that LoRA’s convergence is significantly slower compared to full fine-tuning. To address this issue, researchers have proposed several LoRA variants, such as LoRA+ (Hayou et al., 2024), PISSA (Meng et al., 2024), and LoRA-GA(Wang et al., 2024). These methods have all brought unexpected improvements. By adopting different initialization strategies to influence the model’s training gradients, they have accelerated LoRA’s convergence speed.

Different initializations of LoRA variants accelerate convergence essentially by increasing the initial gradients during training or aligning them with the full-scale training gradients. However, this also makes the initialization process significantly more complex, leading to increased initialization time overhead. To address the issue of complexity and explore the specific reasons for LoRA’s slow convergence, we conducted extensive experiments on initial gradient testing. Ultimately, we concluded that LoRA’s slow convergence is

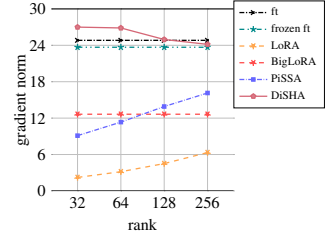


Figure 1. the initial gradient norm of model training.

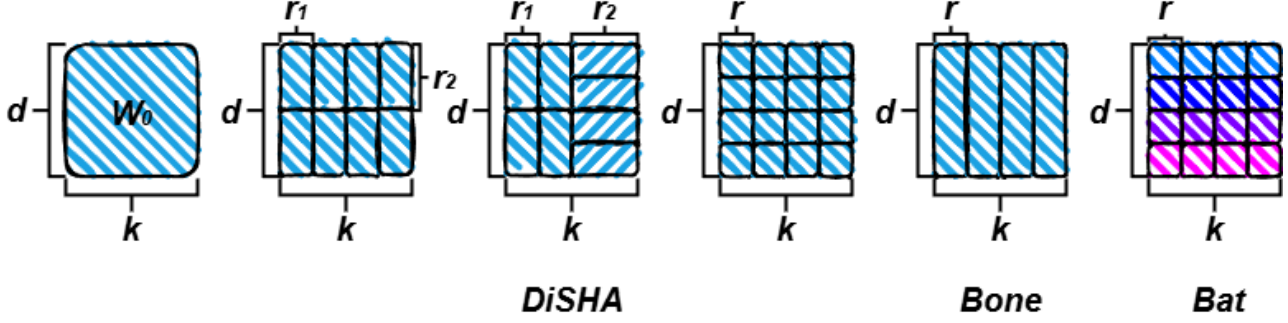


Figure 2. partition of weight matrix W_0 .

influenced not only by initialization but also by its inherent structural limitations. A simpler update structure may be more suitable for fine-tuning LLMs.

Based on the aforementioned conjecture, we first propose a framework with a simpler update mechanism, called Dimension-Sharding Adaptation (DiSHA), designed to achieve larger initial gradients with fewer trainable parameters, thereby accelerating the convergence process. In DiSHA, the pre-trained weight matrix W_0 is frozen and partitioned into multiple shard matrices during training, and all shard matrices share a trainable matrix of the same size as a shard to perform updates, significantly reducing the number of trainable parameters. The design space of DiSHA is extensive, permitting the division of pre-trained weights matrix into dimensions of arbitrary magnitudes, as illustrated in Figure 2. Computational efficiencies vary among design choices, so we proposed an efficient and unified structure named Block Affine Efficient Computation (Bone) within a subset of the DiSHA design space and validated its effectiveness through extensive experiments. As the experiments progressed, we discovered that when fine-tuning with Bone, the updates between different shards within the same matrix are collinear; therefore, to introduce nonlinear updates, we proposed the Block Affine Transformation (Bat) method. Inspired by methods like PiSSA that leverage pre-trained weight matrix information, the updates between different shard matrices are no longer directly added to the trainable matrix. Instead, they need to be linearly transformed with the corresponding shard matrix before being summed. This approach not only leverages the information from the pre-trained weight matrices but also ensures that the updates between different shard matrices become nonlinear.

Our extensive evaluation shows that Bone demonstrates excellent performance on both Natural Language Understanding (NLU) and Natural Language Generation (NLG) tasks, significantly surpassing LoRA and its variants. Moreover, as shown in Figure 5, Bone also achieves a significantly faster convergence rate compared to PiSSA. This demonstrates the feasibility of the DiSHA framework. Furthermore, Bone’s unique design not only resolves the unification challenges of the DiSHA framework, allowing seamless adaptation across

different LLM architectures such as LLaMA, RWKV, and Mistral but also enables it to significantly outperform LoRA in both computational efficiency and memory usage. In NLG tasks, Bone demonstrates superior performance, with evaluation metrics surpassing even the strong LoRA variant Pissa across the board. To verify the feasibility of Bone, we conducted experiments on two different LLM architectures (LLaMA2 (Xu et al., 2023), RWKV6 (Peng et al., 2024)). Based on the comparative experiments between Bone and Bat, it is evident that the non-linear updates of weight shards enhance the model’s performance ceiling.

Our contributions can be summarized as follows

1. We propose a novel PEFT framework called DiSHA which significantly reduces the number of trainable parameters.
2. We proposed an efficient and adaptable structure named Bone within a subset of the DiSHA design space and validated its effectiveness through extensive experiments.
3. We propose Block Affine Transformation (Bat), which introduces shard-specific nonlinearity by integrating pre-trained weight information, without adding new parameters: A breakthrough to overcome the collinear update bottleneck inherent in both Bone.
4. Through extensive experiments, we validated the effectiveness of DiSHA, Bone, and Bat, achieving state-of-the-art (SOTA) performance.

2. Related Works

The PEFT (Parameter-Efficient Fine-Tuning) techniques are diverse and include approaches like adapter tuning (Houlsby et al., 2019; He et al., 2022; Wang et al., 2022; Pfeiffer et al., 2020), prefix tuning (Liu et al., 2023; Li & Liang, 2021), prompt tuning (Brown, 2020; Liu et al., 2023; Lester et al., 2021; Razdaibiedina et al., 2023; Li & Liang, 2021), LoRA (Hu et al., 2021; Meng et al., 2024; Wang et al., 2024; Si et al., 2024), and layer-freezing methods such as LISA.

LoRA, as one of the most popular PEFT techniques, has

demonstrated that the updates to the weights exhibit a low intrinsic rank during adaptation. In LoRA, for a pre-trained weight matrix $\mathbf{W}_0 \in \mathbb{R}^{d \times k}$, we constrain its update by representing the latter with a low-rank decomposition $\mathbf{W}_0 + \Delta\mathbf{W} = \mathbf{W}_0 + \mathbf{B}\mathbf{A}$, where $\mathbf{B} \in \mathbb{R}^{d \times r}$, $\mathbf{A} \in \mathbb{R}^{r \times k}$, and the rank $r \ll \min(d, k)$. During training, \mathbf{W}_0 is frozen and does not receive gradient updates, while \mathbf{A} and \mathbf{B} contain trainable parameters. Note both \mathbf{W}_0 and $\Delta\mathbf{W} = \mathbf{B}\mathbf{A}$ are multiplied with the same input, and their respective output vectors are summed coordinate-wise. For $h = \mathbf{W}_0x$, our modified forward pass yields:

$$h = \mathbf{W}_0x + \Delta\mathbf{W}x = \mathbf{W}_0x + \mathbf{B}\mathbf{A}x \quad (1)$$

Since \mathbf{A} and \mathbf{B} are initialized with Gaussian noise and zeros in LoRA, the gradients can be very small, leading to slow convergence in the fine-tuning process. As a result, many LoRA variants have emerged, aiming to enhance LoRA’s capabilities by modifying the initialization or initial learning rate, among other approaches.

2.1. Adjusting the initial learning rate of LoRA

LoRA+ extended this method by introducing independent learning rates for matrices \mathbf{A} and \mathbf{B} with a fixed ratio, improving the method’s efficiency. DoRA (Liu et al., 2024b) decomposes the weight matrix into two parts: magnitude and direction, which are optimized separately. This approach allows for more precise control over the learning rate, making LoRA updates closer to the effect of full fine-tuning.

2.2. Improving the Initialization of LoRA

PiSSA optimizes the compact parameter space by representing the matrices in the model as the product of two trainable matrices, augmented with a residual matrix for error correction. Using Singular Value Decomposition (SVD), PiSSA initializes the dominant singular values and vectors to train these matrices, while keeping the residual matrix static during fine-tuning. OLoRA (Büyükyüz, 2024) leverages QR decomposition to initialize the adaptation matrices during the fine-tuning process, ensuring that these matrices are orthogonal. This orthogonal initialization helps maintain the stability of the parameter space during optimization. LoRA-GA and PiSSA are similar in form, but they differ in that LoRA-GA initializes \mathbf{A} and \mathbf{B} by computing the initial gradient, thereby closely approximating full fine-tuning.

3. Method

3.1. Motivation: Issues with LoRA

We have identified two main limitations of LoRA and its variants: Firstly, LoRA with simple initialization suffers from slow convergence.

Secondly, while LoRA variants accelerate convergence, they also introduce many more complex operations.

Specifically, methods like PiSSA and OLoRA, which set the initialization by decomposing the pre-trained weights, increase the initialization time. Moreover, the initialization time grows as the model’s parameter size increases.

3.2. DiSHA: Dimension-Sharding Adaptation

To address these limitations and based on the conclusions from the gradient norm experiments A.1, we designed a novel framework called **Dimension-Sharding Adaptation (DiSHA)** to unlock lower trainable parameters and faster convergence by default. For a pre-trained weight matrix $\mathbf{W}_0 \in \mathbb{R}^{d \times k}$, we constrain its update by representing the latter with a low-rank decomposition $\mathbf{W} = \mathbf{W}_0 + \Delta\mathbf{W} = \mathbf{W}_0 + \text{expand}(\mathbf{D})$, where $\mathbf{D} \in \mathbb{R}^{r_1 \times r_2}$, $\text{expand}(\mathbf{D}) \in \mathbb{R}^{d \times k}$, and the rank $(r_1, r_2) \ll \min(d, k)$. During training, \mathbf{W}_0 is frozen and does not receive gradient updates, while the trainable matrix \mathbf{D} is initialized to zero, ensuring $\text{expand}(\mathbf{D})$ initially contributes no update to \mathbf{W}_0 . Note both \mathbf{W}_0 and $\Delta\mathbf{W} = \text{expand}(\mathbf{D})$ are multiplied with the same input, and their respective output vectors are summed coordinate-wise. For $y = \mathbf{W}_0x$, where $x \in \mathbb{R}^{b \times l \times k}$, $y \in \mathbb{R}^{b \times l \times d}$, our modified forward pass yields:

$$y = \mathbf{W}_0x + \Delta\mathbf{W}x = \mathbf{W}_0x + \text{expand}(\mathbf{D})x \quad (2)$$

Here, we explain the concept of $\text{expand}(\mathbf{D})$. As shown in the DiSHA structure in Figure 3, we partition \mathbf{W}_0 into multiple shards along the dimension of \mathbf{D} . The \mathbf{D} matrix is then replicated according to the number of shards, and its dimensions are restored to match \mathbf{W}_0 . Finally, the updated shards are summed to update \mathbf{W}_0 .

3.3. DiSHA Design Space

The design space of DiSHA is determined by its partitioned low-rank update mechanism. Given a pre-trained weight $\mathbf{W}_0 \in \mathbb{R}^{d \times k}$, the trainable matrix $\mathbf{D} \in \mathbb{R}^{r_1 \times r_2}$ governs updates through two configurable degrees of freedom:

1. **Rank Selection:** The ranks r_1 and r_2 independently control the parameterization complexity. For example:

- A wide matrix ($d \ll k$) benefits from $r_1 \ll r_2$ to prioritize input-dimension compactness.
- A tall matrix ($d \gg k$) favors $r_1 \gg r_2$ to minimize memory overhead.

2. **Partitioning Strategy:** The output dimension d can be partitioned into N shards with sizes $\{s_1, \dots, s_N\}$, where $\sum_{i=1}^N s_i = d$. Each shard’s update is scaled by a row of \mathbf{D} :

$$\text{expand}(\mathbf{D}) = \bigoplus_{i=1}^N (\mathbf{1}_{s_i} \otimes \mathbf{D}_i) \in \mathbb{R}^{d \times k}$$

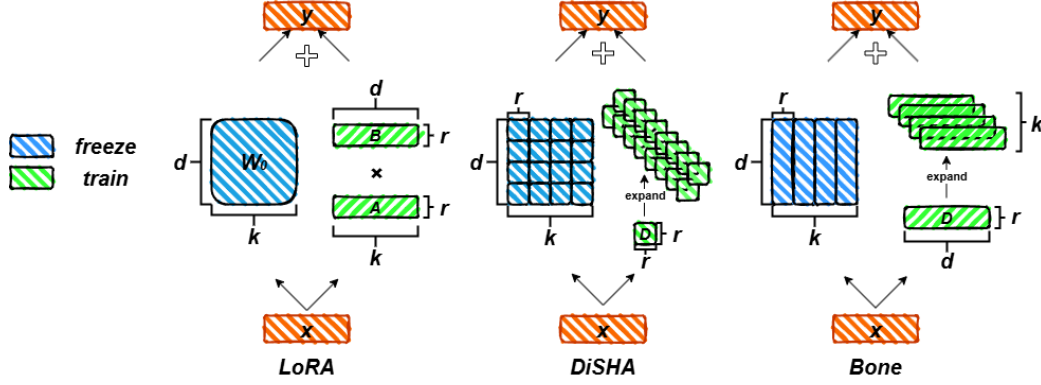


Figure 3. Diagram of LoRA, DiSHA, and Bone Architectures.

Here, $\mathbf{D}_i \in \mathbb{R}^{1 \times r_2}$ is replicated s_i times vertically.

As shown in Table 2, DiSHA can set fewer trainable parameters while supporting non-uniform partitioning (e.g., grouping attention heads in transformers). This allows for a wide design space in DiSHA.

3.4. Bone: Block Affine Efficient Computation

In the previous section, we introduced the DiSHA framework, a method that significantly reduces the number of trainable parameters in the model. Due to the vast design space of the DiSHA framework, it is difficult for users to accurately determine suitable values for training. A good setting of $\mathbf{D} \in \mathbb{R}^{r_1 \times r_2}$ does not generalize well across all neural networks. For example, with the rise of technologies like GQA (Ainslie et al., 2023) and MQA (Shazeer, 2019), the matrix dimensions of self-attention modules ($\mathbf{W}_k, \mathbf{W}_v$) vary greatly among different LLM models.

To enhance the adaptability and efficiency of DiSHA, we proposed **Block Affine Efficient Computation (Bone)**, which reduces the memory footprint of intermediate parameters while enhancing computational efficiency through an innovative input aggregation mechanism.

Core Innovation: Blockwise Input Aggregation Bone redefines the trainable matrix as $\mathbf{D} \in \mathbb{R}^{r \times d}$ with a single rank parameter r , enabling unified adaptation across heterogeneous layers. The key insight is to decouple the input dimension k from the parameterization by introducing **blockwise summation**:

1. **Input Partitioning**: For input $x \in \mathbb{R}^{b \times l \times k}$, partition the k -dimension into r contiguous blocks of size $g = \lfloor k/r \rfloor$:

$$x \rightarrow [x^{(1)}, \dots, x^{(r)}], \quad x^{(i)} \in \mathbb{R}^{b \times l \times g}$$

2. **Blockwise Summation**: Sum each partitioned block

along the k -dimension:

$$\mathbf{S} = \left[\sum_{j=1}^g x_{:, :, j}^{(1)}, \dots, \sum_{j=1}^g x_{:, :, j}^{(r)} \right] \in \mathbb{R}^{b \times l \times r}$$

3. **Affine Projection**: Compute the low-rank update via matrix multiplication with \mathbf{D} :

$$\Delta \mathbf{W}x = \mathbf{D}^\top \mathbf{S} \quad (\mathbf{D} \in \mathbb{R}^{r \times d}, \mathbf{S} \in \mathbb{R}^{b \times l \times r})$$

The final forward pass becomes:

$$y = \mathbf{W}_0 x + \mathbf{D}^\top \mathbf{S}$$

where $\mathbf{D}^\top \mathbf{S} \in \mathbb{R}^{b \times l \times d}$ matches the output dimension of $\mathbf{W}_0 x$.

Mathematical Equivalence to DiSHA Bone’s blockwise summation is equivalent to DiSHA’s $\text{expand}(\mathbf{D})$ operation under structured sparsity. Let $\text{expand}(\mathbf{D}) \in \mathbb{R}^{d \times k}$ be constructed by tiling each row of \mathbf{D} over g columns:

$$\text{expand}(\mathbf{D})_{i,j} = \mathbf{D}_{i, \lceil j/g \rceil}$$

Then:

$$\text{expand}(\mathbf{D})x = \sum_{i=1}^r \mathbf{D}_i \sum_{j=1}^g x_{:, :, j}^{(i)} = \mathbf{D}^\top \mathbf{S}$$

This equivalence allows Bone to avoid explicitly materializing $\text{expand}(\mathbf{D})$, reducing memory from $O(dk)$ to $O(dr)$, and reducing flops from $O(bldk)$ to $O(blr(d + \frac{k}{r}))$.

3.5. Bat: Block Affine Transformation

We conducted extensive experiments on both NLU and NLG tasks to validate the effectiveness of Bone. It outperforms many LoRA variants and surpasses LoRA in terms of memory consumption and computational efficiency. However, we found that Bone results in the updates between different

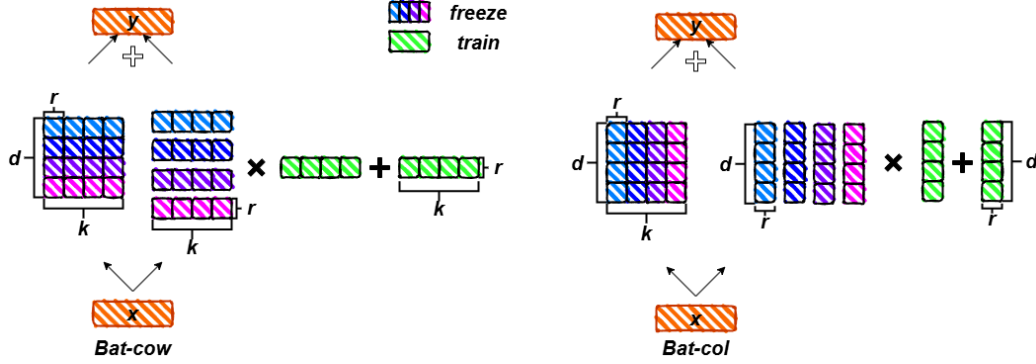


Figure 4. Diagram of Bat Structures in Different Design Spaces.

shards within the same matrix being collinear. Specifically, all shards in the weights use the same trainable matrix for updates, causing the updates of all shards to be collinear, restricting the model’s expressive power. To address the issue of linear correlation among shard updates, our initial idea was to use a trainable coefficient matrix to control the updates of different shards. However, this approach would increase additional parameters.

Inspired by methods like PiSSA that leverage pre-trained weight matrix information, we propose **Block Affine Transformation (Bat)** to break update collinearity without adding parameters. The key insight is to leverage pre-trained weights \mathbf{W}_0 as nonlinear projectors:

1. Tensor Factorization:

- Reshape $\mathbf{W}_0 \in \mathbb{R}^{d \times k}$ into 4D tensor $\mathcal{W}_0 \in \mathbb{R}^{\frac{k}{r} \times \frac{d}{r} \times r \times r}$
- Reshape $\mathbf{D} \in \mathbb{R}^{r \times d}$ into $\mathcal{D} \in \mathbb{R}^{\frac{d}{r} \times r \times r}$

2. **Affine Transformation:** Compute shard-specific updates via tensor contraction:

$$\Delta \mathcal{W} = \mathcal{W}_0 \times_3 \mathcal{D} + \mathcal{D} \in \mathbb{R}^{\frac{k}{r} \times \frac{d}{r} \times r \times r}$$

where \times_3 denotes contraction along the third dimension.

3. **Reconstruction:** Reshape $\Delta \mathcal{W}$ to obtain full update matrix:

$$\Delta \mathbf{W} = \text{Reshape}(\Delta \mathcal{W}) \in \mathbb{R}^{d \times k}$$

Bat allows for flexible configuration of different dimensional transformation strategies based on the settings of \mathbf{D} . For example:

Bat-Row: Reshape \mathbf{W}_0 into $\mathcal{W} \in \mathbb{R}^{\frac{d}{r} \times \frac{k}{r} \times r \times r}$ and $\mathbf{D} \in \mathbb{R}^{r \times k}$ into $\mathcal{D} \in \mathbb{R}^{\frac{k}{r} \times r \times r}$

Bat-Col: Reshape \mathbf{W}_0 into $\mathcal{W} \in \mathbb{R}^{\frac{k}{r} \times \frac{d}{r} \times r \times r}$ and $\mathbf{D} \in \mathbb{R}^{r \times d}$ into $\mathcal{D} \in \mathbb{R}^{\frac{d}{r} \times r \times r}$

The term $\mathcal{W}_0 \times \mathcal{D}$ introduces shard-dependent perturbations proportional to \mathbf{W}_0 ’s singular vectors, breaking the collinearity enforced by Bone’s shared \mathbf{D} . As shown in Table 7, Bat enhances the model’s performance.

4. Experiments

In this section, we evaluate the performance of Bone on various benchmark datasets. Initially, we assess Natural Language Understanding (NLU) capabilities using a subset of the GLUE dataset with the robert-base model. Subsequently, we evaluated the Natural Language Generation (NLG) capabilities by fine-tuning the LLM.

The experiments were conducted on 4×NVIDIA 4090 24G GPUs.

4.1. Experiments on Natural Language Understanding

Models and Datasets We fine-tune the RoBERTa-base model on several datasets from the GLUE benchmark, including MNLI, SST-2, CoLA, QNLI, and MRPC. Performance is evaluated on the development set using accuracy as the primary metric.

Implementation Details The experimental hyperparameter settings were aligned with those in the LoRA repository, but training was conducted using a single 4090 GPU. Each experiment is conducted with 3 different random seeds, and the average performance is reported.

Results As shown in Table 1, Bone demonstrates outstanding performance, particularly on the CoLA dataset, where it exhibits significantly faster convergence and superior data-fitting capabilities, far surpassing LoRA and Pissa.

4.2. Experiment on Natural Language Generation

Models and Datasets To verify the generalizability of Bone, we conducted more comprehensive experiments on LLM. we conducted 3 more task finetuning experiments on LLM: *math*, *code*, and *chat*.

1. *Math*: We trained our model on a 395k subset of MetaMathQA (Yu et al., 2023), a dataset bootstrapped from other math instruction tuning datasets like GSM8K (Cobbe et al.,

Table 1. The results of fine-tuning RoBERTa-base using Bone and various LoRA variants were compared on a subset of the GLUE benchmark.

Method	Trainable	MNLI	SST-2	CoLA	QNLI	MRPC
LoRA	0.236%	85.63 \pm 0.01	94.03 \pm 0.02	62.40 \pm 0.71	91.37 \pm 0.97	87.98 \pm 0.23
Pissa	0.236%	85.72 \pm 0.40	93.64 \pm 0.13	67.28 \pm 0.59	91.40 \pm 0.54	88.11 \pm 0.24
Bone	0.236%	85.71 \pm 0.32	93.60 \pm 0.07	72.86 \pm 3.13	91.43 \pm 0.76	88.14 \pm 0.60

Table 2. We fine-tuned LLMs using Bone and various LoRA variants, and evaluated performance on GSM8k, Math, HumanEval, and MT-Bench.

Model	Strategy	Trainable	GSM8K	Math	HumanEval	MT-Bench
Llama2-7B	LoRA	89.9M	40.75	5.22	17.68	3.73
	OLoRA	89.9M	42.93	6.51	21.12	4.03
	PiSSA	89.9M	43.89	6.92	22.25	4.11
	Bone	87.0M	48.16	8.58	24.08	4.31
RWKV 6-7B	LoRA	88.1M	38.13	6.06	-	-
	PiSSA	88.1M	40.48	6.12	-	-
	Bone	88.1M	41.73	6.52	-	-
Mistral-7B	LoRA	89.1M	65.17	15.82	39.02	-
	PiSSA	89.1M	67.01	18.13	40.85	-
	Bone	88.1M	66.94	18.85	41.76	-

2021) and MATH (Yu et al., 2023), with higher complexity and diversity.

2. Code: We train our model on a 100k subset of Code-Feedback (Zheng et al., 2024b), a high-quality code instruction dataset, removing explanations after code blocks. The model is tested on HumanEval (Chen et al., 2021).

3. Chat: We train our model on a 70k subset of WizardLM-Evol-Instruct (Xu et al., 2024). We test our model on the MT-Bench dataset (Zheng et al., 2024a), which consists of 80 multi-turn questions designed to assess LLMs on multiple aspects. We used GPT-4o to judge the quality of responses, as shown in lm-sys/FastChat.

Implementation Details The hyperparameter settings for this experiment were kept equal, while the train steps were adjusted according to the specific fine-tuning datasets used. It is worth noting that the weights of LLaMA2-7B are not fully symmetric, making it impossible to perfectly align the trainable parameters when comparing Bone and LoRA. To address this, we set the rank r of LoRA to 36 and the rank r of Bone to 64, ensuring that Bone uses fewer parameters than LoRA to demonstrate its superiority. Each experiment is conducted with 2 different random seeds, and the average performance is reported.

Result The results, as shown in Table 2 and Figure 5, demonstrate that Bone outperforms other PEFT methods in terms of convergence speed, data fitting, and generalization capabilities. Bone demonstrates outstanding performance across three different tasks. On LLaMA2-7B, Bone achieves results that surpass Pissa, despite using fewer parameters

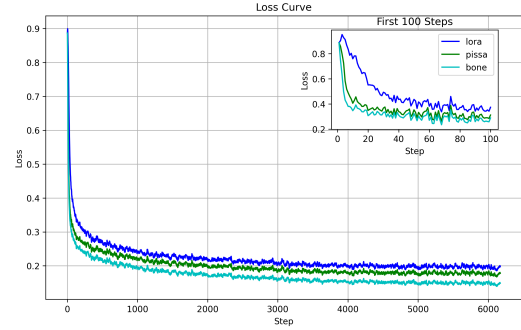


Figure 5. The image shows the loss curve for LLaMA2-7B fine-tuned on the MetaMathQA dataset, with the first 100 steps highlighted for closer observation. Comparing the loss curves reveals that Bone demonstrates superior fitting ability across various architectures and parameter settings. Additionally, Bone exhibits a rapid decrease in loss within the first 100 steps, highlighting its effectiveness.

than LoRA and its variants. On RWKV6-7B, Bone and LoRA have the same number of trainable parameters, yet Bone consistently outperforms LoRA and its variants across all tasks.

4.3. Effect of Rank r

This subsection explores the upper limits of the Bone structure by varying the rank r in the Bone matrix. Comparative experiments were conducted by fine-tuning LLaMA2-7B on the MetaMathQA dataset and validating on GSM8K and Math benchmarks. The test results, as shown in Table 3, demonstrate that the fine-tuning performance improves as

the value of b increases. Notably, when $r = 16$, the Bone structure, with only one-quarter of the trainable parameters compared to PiSSA, surpasses PiSSA’s performance on the GSM8k benchmark. However, its performance on the Math benchmark is only 3.73. The GSM8K score surpasses that of PiSSA, but the Math score is significantly lower, indicating The size of r impacts the model’s ability to understand unseen data. Based on this observation, we hypothesize that when the rank is too small, it significantly limits the model’s generalization ability.

Table 3. Comparing different values of rank (r)

Model	rank	Trainable	GSM8K	Math
Llama2-7B	16	21.7M	45.90	3.77
	32	43.5M	46.18	7.43
	64	87.0M	48.16	8.58
	128	174.0M	53.49	10.08

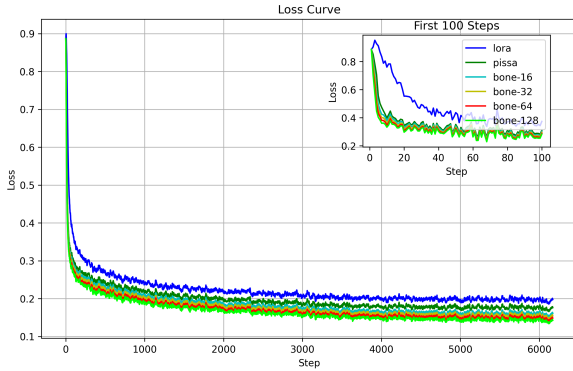


Figure 6. Training loss curves of Bone with different rank r on the MetaMathQA dataset.

4.4. Bone vs Bat

In this section, we have verified the effectiveness of non-linear updates by comparing the performance of Bone and Bat, we fine-tuned LLaMA2-7B and RWKV6-7B using both Bone and Bat on the MetaMathQA dataset and evaluated their performance on Math and GSM8K. As shown in the table, with the same number of trainable parameters, the metrics of non-linear updates are better, successfully breaking the original limits.

Table 4. Comparing Bone, Bat on math tasks

Model	Strategy	Trainable	GSM8K	Math
Llama2-7B	Bone	87.0M	48.16	8.58
	Bat	87.0M	49.36	8.88
RWKV6-7B	Bone	55.1M	41.73	6.52
	Bat	55.1M	42.76	6.60

4.5. Ablation experiments on different grouping methods for Bat

In this subsection, we explore the impact of different grouping methods in the Bat structure on model fine-tuning performance. Due to structural differences in the weight matrix

W , the Bat-free grouping requires manual configuration, which is inconvenient. Therefore, this subsection only compares row-wise and column-wise grouping, both of which can be easily extended to any structure. We fine-tuned LLaMA2-7B on the MetaMathQA dataset and validated the results on GSM8k and Math. The results are shown in Table 5. Since in LLaMA2-7B, the dimension of gate-proj in the MLP part is (4096, 11008), this leads to an asymmetry between row-wise and column-wise grouping in the Bat structure, making it difficult to align parameter counts. Although Bat-row uses 15M fewer parameters than Bat-col, it still delivers excellent performance. However, this discrepancy in parameter counts makes it challenging to accurately evaluate the differences between the grouping methods.

To explore the differences between the two grouping methods and the effect of parameter count, we added a comparative experiment with RWKV6-3B, as RWKV6’s symmetrical structure ensures that the trainable parameter count is the same whether using row-wise or column-wise grouping during Bat fine-tuning. This allows for a fairer comparison between Bat-row and Bat-col.

Table 5. Comparing Bat-row, Bat-col on math tasks

Model	Strategy	Trainable	GSM8K	Math
Llama2-7B	Bat-row	72.8M	45.76	7.82
	Bat-col	87.0M	49.36	8.88
RWKV6-3B	Bat-row	55.1M	25.93	3.12
	Bat-col	55.1M	25.25	3.09

5. Resource and efficiency

The experimental results, shown in Table 5, indicate that the difference between the two is minimal, with both performing well. Therefore, we believe that Bat can effectively fit data regardless of the grouping method used. The key factor influencing Bat’s performance remains the block size. However, this doesn’t imply that different grouping methods are meaningless. As more LLMs begin to use techniques like GQA and MLA (Liu et al., 2024a) to reduce KV cache overhead (Dai et al., 2024; Lee et al., 2024; Shazeer, 2019), the main weight matrices become smaller, and Bat will need to adjust its grouping or employ other techniques to adapt to these new technologies.

Table 6 compares the training resources and token throughput required for fine-tuning RWKV6 using LoRA, Bone, and Bat on a single 4090 GPU. The specific fine-tuning settings are as follows: batch size = 1, context length (ctx_len) = 512.

The results show that Bone has the highest computational efficiency, being nearly 10% faster than LoRA while also being more memory-efficient. However, Bat incurs significantly higher memory usage due to large intermediate values

and is slower in comparison.

At the end of the table, we provide the actual resource costs for fine-tuning RWKV6 on the MetaMathQA dataset using 4 NVIDIA 4090 GPUs, with checkpoint techniques applied.

Table 6. Resource and efficiency

devices	Strategy	Trainable	Memory	throughput
1*gpu	LoRA	55.1M	12074 MB	3.62 kt/s
	Bone	55.1M	11052 MB	3.99 kt/s
	Bat	55.1M	22978 MB	2.16 kt/s
4*gpu	LoRA	55.1M	4*15328 MB	15.6 kt/s
	Bone	55.1M	4*15304 MB	16.0 kt/s
	Bat	55.1M	4*15305 MB	14.2 kt/s

6. Conclusion

In this work, we proposed the DiSHA framework, which divides pre-trained weights into multiple shards and updates them using a shared trainable matrix. This approach significantly reduces resource overhead and opens up new directions for PEFT techniques. To enhance the adaptability and efficiency of DiSHA, we proposed Block Affine Efficient Computation (Bone). Extensive experiments demonstrated the superiority of Bone, which outperforms LoRA and its variants in evaluation metrics, computational efficiency, and resource usage. Bat breakthrough to overcome the collinear update bottleneck inherent in both DiSHA and Bone. By integrating pre-trained weight information through linear transformation. Bat induces nonlinearly independent shard updates without extra parameters.

Collectively, our framework redefines the design principles of efficient adaptation: DiSHA provides theoretical grounding for dimension-wise decomposition, Bone delivers practical efficiency parity with LoRA, and Bat unlocks higher-order update diversity previously unattainable in low-rank methods. This progression demonstrates that parameter efficiency need not come at the cost of expressivity, paving the way for adaptive fine-tuning in resource-constrained environments.

7. Future work

Due to the limitations of the experimental equipment, we did not report any results from the full-scale training required for this work. However, through extensive evaluations and comparisons with LoRA and its variants, we validated the effectiveness of DiSHA, Bone, and Bat. The outstanding performance demonstrated in LLMs by this work gives us great confidence. We believe that DiSHA, Bone, and Bat can be applied to any multimodal task. Of course, this work also has some limitations that need to be addressed. Although Bat successfully overcomes the limitations of Bone, it also

leads to reduced computational efficiency and increased resource consumption. Therefore, in the future, we plan to develop specialized optimized operators to address this issue.

We welcome the community to provide additional suggestions and conduct further tests.

8. Acknowledgments

I would like to express my heartfelt gratitude to all the seniors who provided valuable feedback on my work. Their insightful suggestions have greatly enhanced the quality of this paper. I also wish to thank RWKVOS for their support. Finally, I sincerely appreciate the meticulous guidance provided by the anonymous online mentor, Professor Cormen, whose help has been indispensable.

References

- Ainslie, J., Lee-Thorp, J., de Jong, M., Zemlyanskiy, Y., Lebrón, F., and Sanghai, S. Gqa: Training generalized multi-query transformer models from multi-head checkpoints. *arXiv preprint arXiv:2305.13245*, 2023.
- Biderman, D., Ortiz, J. G., Portes, J., Paul, M., Greengard, P., Jennings, C., King, D., Havens, S., Chiley, V., Frankle, J., et al. Lora learns less and forgets less. *arXiv preprint arXiv:2405.09673*, 2024.
- Brown, T. B. Language models are few-shot learners. *arXiv preprint ArXiv:2005.14165*, 2020.
- Büyükakyüz, K. Olora: Orthonormal low-rank adaptation of large language models. *arXiv preprint arXiv:2406.01775*, 2024.
- Chen, M., Tworek, J., Jun, H., Yuan, Q., de Oliveira Pinto, H. P., Kaplan, J., Edwards, H., Burda, Y., Joseph, N., Brockman, G., Ray, A., Puri, R., Krueger, G., Petrov, M., Khlaaf, H., Sastry, G., Mishkin, P., Chan, B., Gray, S., Ryder, N., Pavlov, M., Power, A., Kaiser, L., Bavarian, M., Winter, C., Tillet, P., Such, F. P., Cummings, D., Plappert, M., Chantzis, F., Barnes, E., Herbert-Voss, A., Guss, W. H., Nichol, A., Paino, A., Tezak, N., Tang, J., Babuschkin, I., Balaji, S., Jain, S., Saunders, W., Hesse, C., Carr, A. N., Leike, J., Achiam, J., Misra, V., Morikawa, E., Radford, A., Knight, M., Brundage, M., Murati, M., Mayer, K., Welinder, P., McGrew, B., Amodei, D., McCandlish, S., Sutskever, I., and Zaremba, W. Evaluating large language models trained on code, 2021.
- Cobbe, K., Kosaraju, V., Bavarian, M., Chen, M., Jun, H., Kaiser, L., Plappert, M., Tworek, J., Hilton, J., Nakano, R., Hesse, C., and Schulman, J. Training verifiers to solve math word problems. *arXiv preprint arXiv:2110.14168*, 2021.
- Dai, J., Huang, Z., Jiang, H., Chen, C., Cai, D., Bi, W., and Shi, S. Sequence can secretly tell you what to discard. *arXiv preprint arXiv:2404.15949*, 2024.
- Ding, N., Qin, Y., Yang, G., Wei, F., Yang, Z., Su, Y., Hu, S., Chen, Y., Chan, C.-M., Chen, W., et al. Parameter-efficient fine-tuning of large-scale pre-trained language models. *Nature Machine Intelligence*, 5(3):220–235, 2023.
- Hayou, S., Ghosh, N., and Yu, B. Lora+: Efficient low rank adaptation of large models. *arXiv preprint arXiv:2402.12354*, 2024.
- He, J., Zhou, C., Ma, X., Berg-Kirkpatrick, T., and Neubig, G. Towards a unified view of parameter-efficient transfer learning, 2022.
- Houlsby, N., Giurgiu, A., Jastrzebski, S., Morrone, B., De Laroussilhe, Q., Gesmundo, A., Attariyan, M., and Gelly, S. Parameter-efficient transfer learning for nlp. In *International conference on machine learning*, pp. 2790–2799. PMLR, 2019.
- Hu, E. J., Shen, Y., Wallis, P., Allen-Zhu, Z., Li, Y., Wang, S., Wang, L., and Chen, W. Lora: Low-rank adaptation of large language models. *arXiv preprint arXiv:2106.09685*, 2021.
- Lee, W., Lee, J., Seo, J., and Sim, J. {InfiniGen}: Efficient generative inference of large language models with dynamic {KV} cache management. In *18th USENIX Symposium on Operating Systems Design and Implementation (OSDI 24)*, pp. 155–172, 2024.
- Lester, B., Al-Rfou, R., and Constant, N. The power of scale for parameter-efficient prompt tuning, 2021.
- Li, X. L. and Liang, P. Prefix-tuning: Optimizing continuous prompts for generation. *arXiv preprint arXiv:2101.00190*, 2021.
- Liu, A., Feng, B., Wang, B., Wang, B., Liu, B., Zhao, C., Dengr, C., Ruan, C., Dai, D., Guo, D., et al. Deepseek-v2: A strong, economical, and efficient mixture-of-experts language model. *arXiv preprint arXiv:2405.04434*, 2024a.
- Liu, S.-Y., Wang, C.-Y., Yin, H., Molchanov, P., Wang, Y.-C. F., Cheng, K.-T., and Chen, M.-H. Dora: Weight-decomposed low-rank adaptation. *arXiv preprint arXiv:2402.09353*, 2024b.
- Liu, X., Zheng, Y., Du, Z., Ding, M., Qian, Y., Yang, Z., and Tang, J. Gpt understands, too. *AI Open*, 2023.
- Meng, F., Wang, Z., and Zhang, M. Pissa: Principal singular values and singular vectors adaptation of large language models. *arXiv preprint arXiv:2404.02948*, 2024.
- Peng, B., Goldstein, D., Anthony, Q., Albalak, A., Alcaide, E., Biderman, S., Cheah, E., Ferdinan, T., Hou, H., Kazienko, P., et al. Eagle and finch: Rwkv with matrix-valued states and dynamic recurrence. *arXiv preprint arXiv:2404.05892*, 2024.
- Pfeiffer, J., Kamath, A., Rücklé, A., Cho, K., and Gurevych, I. Adapterfusion: Non-destructive task composition for transfer learning. *arXiv preprint arXiv:2005.00247*, 2020.
- Radford, A., Wu, J., Child, R., Luan, D., Amodei, D., Sutskever, I., et al. Language models are unsupervised multitask learners. *OpenAI blog*, 1(8):9, 2019.
- Raffel, C., Shazeer, N., Roberts, A., Lee, K., Narang, S., Matena, M., Zhou, Y., Li, W., and Liu, P. J. Exploring

the limits of transfer learning with a unified text-to-text transformer. *Journal of machine learning research*, 21 (140):1–67, 2020.

Razdaibiedina, A., Mao, Y., Hou, R., Khabsa, M., Lewis, M., Ba, J., and Almahairi, A. Residual prompt tuning: Improving prompt tuning with residual reparameterization, 2023.

Shazeer, N. Fast transformer decoding: One write-head is all you need. *arXiv preprint arXiv:1911.02150*, 2019.

Si, C., Wang, X., Yang, X., Xu, Z., Li, Q., Dai, J., Qiao, Y., Yang, X., and Shen, W. Flora: Low-rank core space for n-dimension. *arXiv preprint arXiv:2405.14739*, 2024.

Wang, S., Yu, L., and Li, J. Lora-ga: Low-rank adaptation with gradient approximation. *arXiv preprint arXiv:2407.05000*, 2024.

Wang, Y., Agarwal, S., Mukherjee, S., Liu, X., Gao, J., Awadallah, A. H., and Gao, J. Adamix: Mixture-of-adaptations for parameter-efficient model tuning. *arXiv preprint arXiv:2205.12410*, 2022.

Xu, C., Sun, Q., Zheng, K., Geng, X., Zhao, P., Feng, J., Tao, C., Lin, Q., and Jiang, D. Wizardlm: Empowering large pre-trained language models to follow complex instructions. In *The Twelfth International Conference on Learning Representations*, 2024.

Xu, L., Xie, H., Qin, S.-Z. J., Tao, X., and Wang, F. L. Parameter-efficient fine-tuning methods for pretrained language models: A critical review and assessment. *arXiv preprint arXiv:2312.12148*, 2023.

Yu, L., Jiang, W., Shi, H., Yu, J., Liu, Z., Zhang, Y., Kwok, J. T., Li, Z., Weller, A., and Liu, W. Metamath: Bootstrap your own mathematical questions for large language models. *arXiv preprint arXiv:2309.12284*, 2023.

Zheng, L., Chiang, W.-L., Sheng, Y., Zhuang, S., Wu, Z., Zhuang, Y., Lin, Z., Li, Z., Li, D., Xing, E., et al. Judging llm-as-a-judge with mt-bench and chatbot arena. *Advances in Neural Information Processing Systems*, 36, 2024a.

Zheng, T., Zhang, G., Shen, T., Liu, X., Lin, B. Y., Fu, J., Chen, W., and Yue, X. Opencodeinterpreter: Integrating code generation with execution and refinement. *arXiv preprint arXiv:2402.14658*, 2024b.

A. Appendix

A.1. Gradient Norm

To investigate the factors affecting the convergence speed of LLM training, we conducted extensive experiments. In the gradient norm analysis, we observed that a larger initial gradient norm leads to faster loss convergence. Initially, we compared full fine-tuning (FT), LoRA, and PiSSA, as shown in the figure 1 (The figure illustrates the initial gradient norm of model training for different structures at various ranks. Notably, FT (full fine-tuning), Frozen FT, and BigLoRA remain unaffected by rank, as their trainable parameters remain constant.) and figure 5. Many studies suggest that LoRA’s slow convergence speed is likely due to the small gradients caused by the zero initialization of either multiplicand matrix. However, we hypothesize that LoRA’s slow convergence could also be attributed to structural issues. To test this hypothesis, we introduced two additional experiments: Frozen FT and BigLoRA. Both experiments freeze the pre-trained weights \mathbf{W}_0 , but they differ in design. Frozen FT replaces \mathbf{W}_0 with a trainable matrix \mathbf{W}_t of the same dimensions, initialized to zero. BigLoRA, on the other hand, sets the rank to 1024, ensuring that its trainable parameter count exceeds both Frozen FT and FT.

We observed an intriguing phenomenon: although the initial gradient norm of LoRA and PiSSA increases with larger ranks, BigLoRA, despite having significantly more trainable parameters than Frozen FT or FT, still only has an initial gradient norm of 12.64. Meanwhile, Frozen FT, despite being initialized to zero, has an initial gradient norm only slightly smaller than FT. This suggests that there may be simpler structural solutions that can naturally unlock lower intrinsic ranks and achieve faster convergence without the need for additional complexity. Finally, we added the initial gradient data of Bone to represent the performance of the DiSHA framework.

A.2. Efficiency Analysis

Table 7. Comparing Bone, Bat on math tasks

Operation	Memory Complexity	FLOPs
LoRA ($\mathbf{B}\mathbf{A}x$)	$O(dr + rk)$	$O(blr(d + k))$
DiSHA (expand(\mathbf{D}) x)	$O(dk)$	$O(bldk)$
Bone ($\mathbf{D}^\top \mathbf{S}$)	$O(dr)$	$O(blr(d + \frac{k}{r}))$

•**Memory Reduction:** Bone saves $\frac{k}{r}$ memory over DiSHA when $r \ll k$.

•**FLOPs Advantage:** Bone’s blockwise summation replaces $O(bldk)$ dense multiplication with $O(blk)$ summation and $O(bldr)$ projection, achieving up to 2.0× speedup (see Table 6).